Korea-Australia Rheology Journal
Vol. 17, No. 3, September 2005 pp. 117-123

Hemorheology and clinical application : association of impairment of red blood cell deformability with diabetic nephropathy

Sehyun Shin* and Yunhee Ku
School of Mechanical Engineering, Kyungpook National University
(Received April 27, 2005)

Abstract

Background: Reduced deformability of red blood cells (RBCs) may play an important role on the pathogenesis of chronic vascular complications of diabetes mellitus. However, available techniques for measuring RBC deformability often require washing process after each measurement, which is not optimal for day-to-day clinical use at point of care. The objectives of the present study are to develop a device and to delineate the correlation of impaired RBC deformability with diabetic nephropathy.
Methods: We developed a disposable ektacytometry to measure RBC deformability, which adopted a laser diffraction technique and slit rheometry. The essential features of this design are its simplicity (ease of operation and no moving parts) and a disposable element which is in contact with the blood sample. We studied adult diabetic patients divided into three groups according to diabetic complications. Group I comprised 57 diabetic patients with normal renal function. Group II comprised 26 diabetic patients with chronic renal failure (CRF). Group III consisted of 30 diabetic subjects with end-stage renal disease (ESRD) on hemodialysis. According to the renal function for the diabetic groups, matched non-diabetic groups were served as control.
Results: We found substantially impaired red blood cell deformability in those with normal renal function (group I) compared to non-diabetic control ($P = 0.0005$). As renal function decreases, an increased impairment in RBC deformability was found. Diabetic patients with chronic renal failure (group II) when compared to non-diabetic controls (CRF) had an apparently greater impairment in RBC deformability ($P = 0.07$). The non-diabetic cohort (CRF), on the other hand, manifested significant impairment in red blood cell deformability compared to healthy control ($P = 0.0001$).
Conclusions: The newly developed slit ektacytometer can measure the RBC deformability with ease and accuracy. In addition, progressive impairment in cell deformability is associated with renal function loss in all patients regardless of the presence or absence of diabetes. In diabetic patients, early impairment in RBC deformability appears in patients with normal renal function.

Keywords **:** disposable, ektacytometry, RBC, deformability, diabetes, nephropathy

1. Introduction

Blood is amazing fluid in various aspects. From a biological point of view, blood can be considered as a tissue comprising various types of cells and a liquid intercellular material. From a rheological point of view, blood can be thought of as a two-phase liquid; it can also be considered as a solid-liquid suspension, with the cellular elements being the solid phase. However, blood can also be considered as a liquid-liquid emulsion based on the liquid-like behavior of red blood cells (RBCs) under shear. Blood is a concentrated suspension of formed elements including red blood cells (RBCs) or erythrocytes, white blood cells (WBCs) or leukocytes and platelets. The suspending fluid, the blood plasma, is an aqueous solution containing numerous chemical species, from ions to macro-molecules. Normal blood has a volume concentration of RBCs (hematocrit) 40% to 45%. The present study discusses the RBC deformability and its association with clinical observations.

In fact, RBCs have ability to undergo large deformations when subjected to stresses, which allows the RBCs to pass through capillaries narrower than resting RBC diameter. RBCs are biconcave discs typically 6-8 μm in diameter and 2 μm in thickness; in mammals the cells are non-nucleated and consist of a concentrated hemoglobin solution enveloped by a highly flexible membrane. A slight decrease in red cell deformability may cause important disturbances in the blood circulation of micro-vessels. Fig. 1 shows the significance of RBC deformability on blood vis-

*Corresponding author: shins@knu.ac.kr

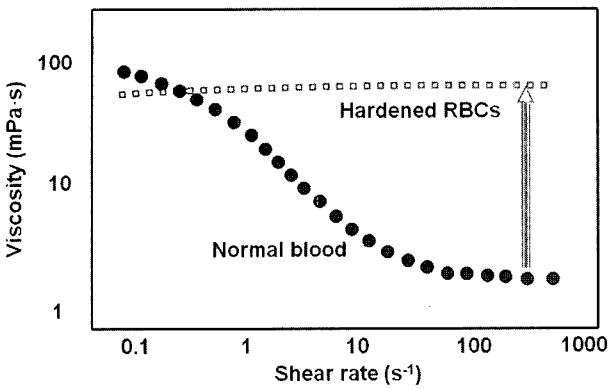

Fig. 1. Effect of red blood cell deformability on blood viscosity.

cosity (Chien, 1970). In Fig. 1, reduced RBC deformability causes a significant increase of blood viscosity over a range of shear rates. Recent clinical observations have reported that reduced RBC deformability accompany diabetes (Garnier *et al.*, 1990; Testa *et al.*, 2003; Brown *et al.*, 2005), hypertension (Vaya *et al.*, 1992), sickle cell anemia (Huang *et al.*, 2003; Usami *et al.*, 1975) and other circulation disorders. The chronic consequences of such diseases exclusively, or to a great extent, afflict the microcirculation and cause vascular complications. Diabetic nephropathy, which is one of the serious microvascular complications of diabetes mellitus, is the major cause of renal diseases including chronic renal failure (CRF) and end-stage renal disease (ESRD) (Mauer *et al.*, 1985). The progressive mechanism of these vascular complications has been rarely known. However, hyperglycemia is the main metabolic perturbation causing irreversible damage to kidney for diabetes (Porte *et al.*, 1996). Due to the exponential increase of diabetic vascular complications, there has been required to investigate the correlation of RBC deformability with diabetic nephropathy.

Various techniques for measuring the deformability of RBCs have been proposed and comparisons regarding their effectiveness can be found elsewhere (Bareford *et al.*, 1985; Caimi *et al.*, 2004). Typical techniques can be summarized briefly as follows: (i) *RBC filtration*: This method has been widely used in measuring RBC deformability due to its similarity and simplicity (Hanss, 1983; Baskurt *et al.*, 1996). Deformability can be determined by measuring either the pressure build-up across the membrane during a test period or the transit time related to a certain number of RBCs. However, there is a major drawback to this method in that a calibration standard is lacking. Other methods such as micropipette aspiration have also been used to measure RBC deformability; (ii) *Rheoscope* (Schmid-Schönbein *et al.*, 1969; Dobbe *et al.*, 2002; Dobbe *et al.*, 2004): This involves direct observation of the shape of RBCs under a given shear stress. This method allows researchers to confirm the tank treading of RBCs in shear flow. (iii) *Ektacytometry* (Hardemann *et al.*, 1994; Schmid-Schonbein *et al.*, 1996): This technique uses laser diffraction analysis of RBCs under varying stress levels. This method has several advantages compared to other techniques, in that it is relatively easy to perform, has acceptable precision, and can be performed at various shear stresses. Recently, ektacytometers have been further developed and are commercially available in models such as LORCA®(R&R Mechatronics, Hoorn, Netherlands) and RHEODYN SSD (Myrenne, Roetgen, Germany).

Although there are many methods and instruments for measuring deformability as described above, most of the current techniques including ektacytometry require cleaning after each measurement. In order to measure cell deformability in a clinical setting, one needs to repeat the cleaning after each measurement, which is a labor-intensive and time-consuming process. Hence, current techniques are not optimal for day-to-day clinical use. Therefore, there has been a need to develop a simple and labor-free disposable element which eliminates frequent cleaning. Recently, our previous study (Shin *et al.*, 2005) developed a new disposable-slit ektacytometer (RheoscanD), which is capable of continuously measuring RBC deformability over a broad range of shear stresses. The principle of the proposed slit ektacytometer is based on the combination of the laser-diffraction technique and a disposable slit rheometry. Throughout the development of this technique emphasis has been placed on the simplicity of the measuring process, i.e., designing of a disposable element that holds the blood sample, so that the present technique can be applicable in the clinical environment. Therefore, the objective of the present study is to investigate the correlation of the reduced RBC deformability with progressive development of diabetic nephropathy using the disposable ektacytometry.

2. Method and materials

2.1. Subjects

One hundred and thirteen diabetic patients, divided into three groups according to serum creatinine concentration. Forty (normal, healthy), fifty one (CRF) and forty (ESRD) nondiabetic patients served as controls. The detailed statistical data are available in Table 1 including group designation, patient's demographics, and clinical data. Group-I comprised 57 diabetic patients whose serum creatinine was less than 1.5 mg/dL. Group-II comprised 26 diabetic patients with renal insufficiency (CRF) whose serum creatinine ranged from 2 to 6 mg/dL and Group-III comprised of 30 diabetic patients with ESRD whose serum creatinine ranged from 7 to 16 mg/dL. In nondiabetic cohort, 40 healthy controls having normal renal function, 51 patients with CRF and 40 with ESRD were controls for diabetic groups I, II and III, respectively. No patients in the non-

Table 1. Patient demographics and clinical features

	Healthy (n=40)	Normal renal function (n=57)	Chronic renal failure (n=77)		End stage renal disease (n=70)	
	Group 0 Healthy (40)	Group I Diabetic (57)	Group II Diabetic (26)	Control Non-Diabetic (51)	Group III Diabetic (30)	Control Non-Diabetic (40)
Age	47.1 ± 10.2	59.9 ± 12.9	59.0 ± 13.9	56.4 ± 11.0	52.1 ± 14.3	50.7 ± 15.3
Gender (male/female)	19/21	35/22	14/12	32/19	19/11	27/13
Serum Creatinine (mg/dL)		0.81 ± 0.2	4.01 ± 1.54	4.11 ± 1.86	9.02 ± 2.79	9.47 ± 2.28
		< 1.5	2 < x < 6		> 7	

diabetic group have clinically evident cardiovascular diseases.

The samples of venous blood were drawn from the antecubital vein and collected into an EDTA containing Vacutainers (BD, Franklin Lakes, NJ). The blood samples used in the experiments were completed within 6 hours after blood collection. The present method does not require complex multi-step processes to prepare blood samples. Only simply mixing blood with a high viscous liquid is required. The whole blood sample was then mixed with a solution of 0.14 mM Polyvinypyrrolidone (PVP, M = 360 000, Sigma, St. Louis, MO, USA) at the optimal hematocrit of 0.5.

2.2. Apparatus and operating principle

The basic apparatus of the slit ektacytometer (Shin *et al.*, 2005), containing the laser, a CCD video camera, screen, vacuum generating mechanism and pressure driven slit rheometry, is shown in Fig. 2. Typical tests are conducted as follows: At time $t = 0$, the vacuum generating mechanism is connected with the slit element, which allows the fluid to flow through the slit and to be collected in the waste sample chamber as driven by the differential pressure. When the differential pressure reaches equilibrium with a pressure head, the test fluid stops flowing.

While the blood is flowing through the slit, a laser beam emitted from the laser diode traverses the diluted RBC suspension and is diffracted by the RBCs in the volume. The diffraction pattern projected on the screen is captured by a CCD-video camera, which is linked to a frame grabber integrated with a computer. While the differential pressure is decreasing, the RBCs change gradually from a prolate ellipsoid towards a biconcave morphology. The Elongation Index (*EI*) as a measure of the RBC deformability is determined from an isointensity curve in the diffraction pattern using an ellipse-fitting program. It is noteworthy that the diffraction pattern images are oriented perpendicular to the orientation of the elongated cells.

The essential feature of our proposed ektacytometer is the use of a disposable element including the slit. The disposable element can be made of various materials including glass, silicon, and PMMA, etc. The present slit is made of transparent polystyrene using micro-injection molding. Using the disposable element eliminates the labor-intensive and time-consuming washing process after measurements. In fact, the washing process has prevented previous ektacytometers from being used in a clinical setting. However, the proposed disposable-slit ektacytometer by eliminating these problems can be used in a clinical setting.

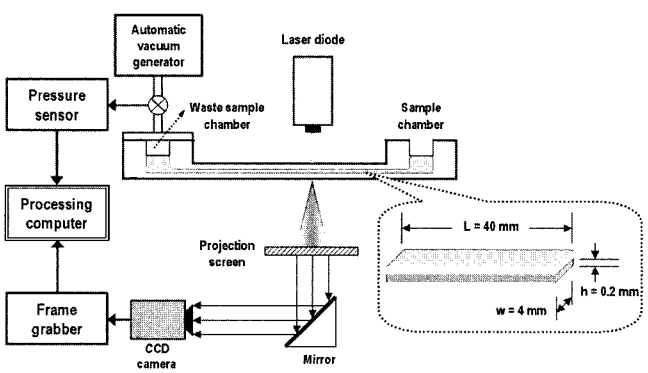

Fig. 2. Schematics of a slit-flow ektacytometry.

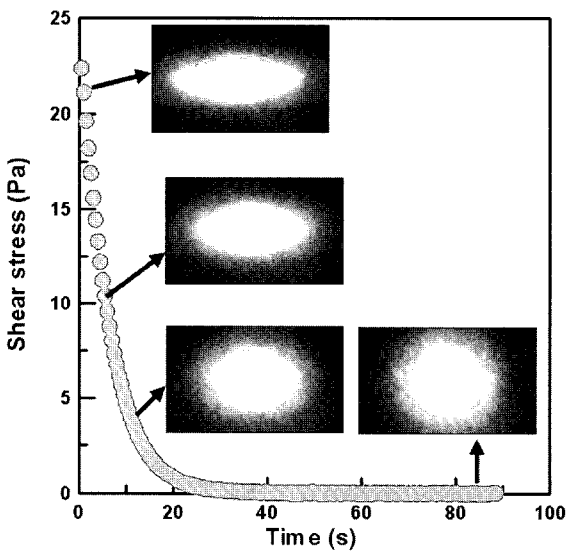

Fig. 3. Shear stress variation and corresponding diffraction images along time.

Fig. 3 shows the shear stress variations over time for the diluted RBC suspension. With time, the shear stress between the waste sample chamber and atmosphere decreases since the waste sample chamber is filled with the flowing fluid from the slit. Typically, it takes approximately one minute to reach an asymptote for the diluted RBC suspension. In fact, the time to complete a run varies depending on the type of liquid and the dimensions of the slit. It is noteworthy that the initial pressure in the vacuum chamber was chosen to produce the maximum shear stress of approximately 30 Pa.

A detailed description of the stress-shear rate relation can be found in a previous study (Shin *et al.*, 2005). A brief description is as follows: In deriving the stress-shear rate relation in the slit rheometer, the important assumptions are 1) a fully developed, isothermal, laminar flow; 2) no slip at the walls; and 3) air in the vacuum chamber as an ideal gas. Assuming that the product of pressure $P(t)$ and volume $V(t)$ in the vacuum chamber at time t is constant, $P_iV_i = P(t)V(t)$, where subscript i represents the initial state of the experiment, the instantaneous Pressure $P(t)$ is recored in the computer file. The flow rate at time t can be obtained as $Q(t) = \frac{d}{dt}\left(\frac{P_iV_i}{P(t)}\right)$. On the other hand, the pressure difference through a slit can be expressed as $P = \{P_A - P(t) - \rho gL\}$ and the corresponding shear stress as $\tau_w(t) = \Delta P(t)h/\{(1 + 2h/w)L\}$. The shear rate at the slit wall is obtained from the classical Weissenberg-Rabinowitsch equation (Macosko, 1993)

$$\dot{\gamma}_w(t) = -\left.\frac{dv_z}{dz}\right|_w = \frac{1}{3}\dot{\gamma}_{aw}\left[2 + \frac{d\ln Q}{d\ln \tau_w}\right] \quad (1)$$

where $\dot{\gamma}_{aw}$ is $6Q/wh^2$.

For calibration purpose of the slit rheometer, water and an aqueous solution of commercial polyacrylamide (Separan AP-273, Dow Chem. Co.) were measured and the results were compared with those measured by a rotating viscometer (Physica model UDS-200, Parr Physica, Inc.) at specific temperatures. Compared with these results, the test results give about a 2.8% error across the entire shear rate range (Shin *et al.*, 2005).

2.3. Laser-diffraction

The basic apparatus of the laser-diffractometer contains the laser diode, a CCD video camera, screen, and the disposable slit, as shown in Fig. 2. The laboratory setup also included a computer. A laser diode (635 nm, 1.5 mW) and a CCD camera (SONY-ES30) combined with a frame grabber were used to obtain a laser-diffraction pattern. The diffraction pattern is analyzed by an ellipse-fitting-program and the elongation indices (EI) are deter-mined at the corresponding shear stresses (0~25 Pa) When the laser beam passes through the test slit, the light is diffracted, forming an image that corresponds to the shape of all the cells that pass the laser beam. As leucocytes differ in shape, they only contribute to the resulting diffraction image by scattering. The same holds true for thrombocytes. In addition, leucocytes and thrombocytes are low in concentration compared to RBC. Thus, the diffraction image represents the mean deformability of all the RBCs that pass the laser beam.

The diffraction pattern projected on the screen is captured by a CCD-video camera, which is linked to a frame grabber integrated with a computer. As the differential pressure decreases, the RBCs change gradually from a prolate ellipsoid towards a biconcave morphology. The captured diffraction images corresponding to the pressure are described in Fig. 3 along time. For image analysis, all image areas with the same intensity are evaluated, thereby forming isointensity lines. The Elongation Index (*EI*) as a measure of RBC deformability is determined from an isointensity curve in the diffraction pattern using an ellipse-fitting program. The elongation index *EI* is defined as $(L-W)/(L+W)$, where L and W are the major and minor axes of the ellipse, respectively.

2.4. Validity and reproducibility

The slit ektacytometer, Rheoscan-D, was tested were compared to the elongation data regarding validity, reproducibility, and errors of measurements for normal red blood cells. The results measured with the commercial rotating type ektacytometry, LORCA (R&R Mechatronics, Netherlands). The test results from the slit ektacytometer, Rheoscan-D, were in close agreement (less than 5%) with those from the rotating ektacytometer in a shear stress range of 0~20 Pa.

Table 2 lists the mean elongation index and the standard deviation at various shear stresses for the 10 subsamples in the reproducibility test. The average deformability of all samples fell inside the 95% confidence intervals of the samples. When the shear stress was higher than 1.0 Pa, the coefficient of variations (CV) of the slit ektacytometer was less than 2.8%. Both instruments show decreasing CV values with an increase in the shear stress. Table 2 shows that in this experiment the mean elongation index (*EI*) obtained with the LORCA ektacytometer was close to that obtained with the slit ektacytometer.

3. Results and discussion

Fig. 4 compares the diffraction images for healthy and diabetic RBCs at various shear stresses. As shown in Fig. 4, the diffraction patterns of the RBCs change gradually from a prolate ellipsoid towards the circular morphology as the shear stress decreases. It is noteworthy that there are differences in the ellipsoid shapes between control and diabetes. For the ellipsoid shapes between control and diabetes. For example, at a given shear stress (τ= 8 Pa), the

Table 2. Mean values of EI for normal RBC measured with Rheoscan-D and LORCA

Rheoscan-D (n = 10)			LORCA (n = 10)		
Shear stress (Pa)	Mean EI ± SD	CV (%)	Shear stress (Pa)	Mean EI ± SD	CV (%)
0.3	1.1 ± 0.5	45.5	0.3	2.3 ± 0.9	39.1
0.5	5.9 ± 0.3	5.1	0.5	6.1 ± 0.6	9.8
1	16.2 ± 0.2	1.2	1	15.1 ± 0.7	4.6
2	26.7 ± 0.5	1.8	2	26.1 ± 0.5	1.9
5	39.8 ± 0.4	1.0	5	39.1 ± 0.3	0.7
10	45.7 ± 0.2	0.4	10	47.5 ± 0.3	0.6
20	50.8 ± 0.2	0.4	20	54.5 ± 0.2	0.3

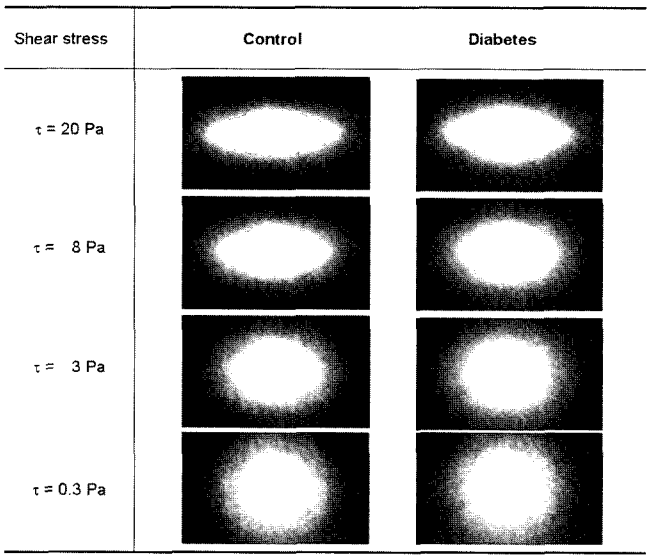

Fig. 4. Laser diffraction patterns at various wall shear stresses for healthy control and diabets.

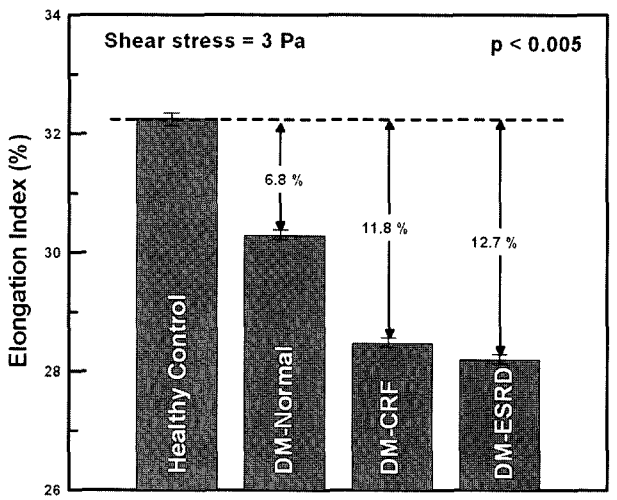

Fig. 5. Comparison of red cell deformability for healthy control and diabetes.

diffraction pattern for controlled RBCs shows the larger deformation than that for the diabetic RBCs. Through the image analysis process, the elongation indexes can be determined and those values can be compared between them. Table 3 shows the detailed value of the elongation indexes for various groups.

Fig. 5 shows the comparison of RBC deformability for healthy and diabetic groups. The diabetic group with normal renal function (group I) shows a substantially greater impairment in red blood cell deformability compared with normal healthy control ($P = 0.004$). Subsequently, a further impaired RBC deformability was found with renal function loss, in diabetic patients with renal insufficiency (group II) when compared with diabetic subjects with normal renal function ($P = 0.008$). In addition, there shows a slight further reduction of RBC deformability when renal function loss progress from CRF (group II) to ESRD (group III). These subsequent decreases of RBC deformability imply that the RBC deformability impairment play a significant role in the progress of diabetic renal diseases. When microvascular vessels are exposed to flowing less deformable RBCs for long period of time, there might cause mechanical damages on the vessel walls and result in either narrowing or hardening process of vessel wall.

Fig. 6 shows the comparison of RBC deformability for healthy and non-diabetic groups. In the nondiabetic cohort, marked impaired red blood cell deformability was also noted in patients with renal insufficiency. The non-diabetic group with renal insufficiency (CRF and ESRD) shows a

Table 3. Comparison of red cell deformability at shear stress of 3 Pa

Shear stress (Pa)	Healthy (n=40)	Diabetes (n=57)	Diabetic CRF (n=26)	CRF (n=51)	Diabetic ESRD (n=30)	ESRD (n=40)	p-value
3Pa	32.3 ± 0.09	30.3 ± 0.08	28.5 ± 0.08	28.7 ± 0.09	28.2 ± 0.08	28.6 ± 0.10	p < 0.005

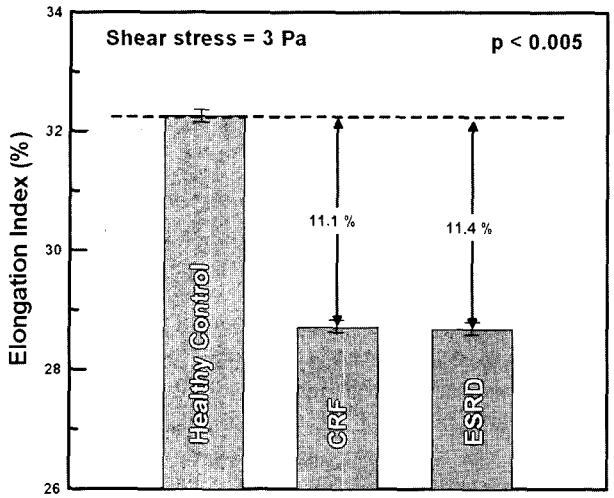

Fig. 6. Comparison of red cell deformability for healthy control and non-diabetic renal diseases.

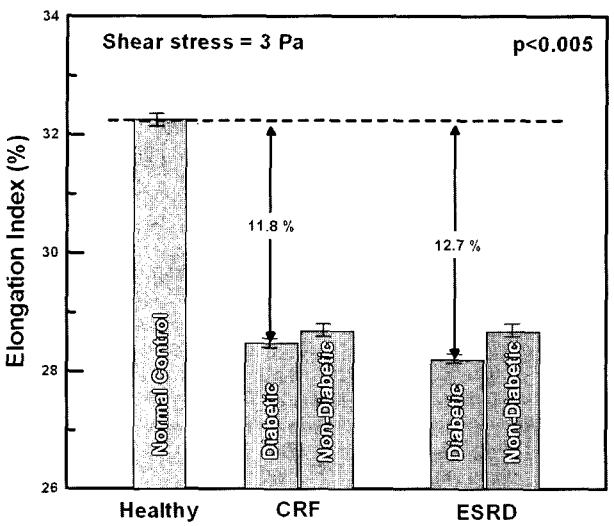

Fig. 7. Comparison of red cell deformability for diabetes and non-diabetic renal diseases.

significant reduction of red blood cell deformability compared with normal healthy control ($P = 0.001$). However, there was no noticeable difference between CRF and ESRD patients.

Fig. 7 shows comparison of RBC deformability for diabetic and non-diabetic groups. The diabetic group with renal insufficiency (group II) shows a slight greater impairment in red blood cell deformability than the non-diabetic group with renal insufficiency ($P = 0.5$). Similarly, the diabetic group with ESRD (group III) shows a slight greater impairment in red blood cell deformability than the non-diabetic group with ESRD ($P = 0.8$). However, the correlation cannot be found between them. This fact implies that the chronic renal diseases can be found when RBC deformability reaches asymptotic minimum value. In other words, the less deformable RBCs may the cause of the microvascular damages while they pass through the capillary smaller than RBCs themselves.

4. Conclusion

Red blood cell deformability in diabetic patients is profoundly altered early, prior to the onset of renal insufficiency and a persistently increased impairment in red blood cell deformability is associated with renal function loss. By contrast, the impairment in red blood cell deformability is initially observed in nondiabetic patients with the onset of renal insufficiency. Red blood cell deformability impairment in either nondiabetic or diabetic patients reaches a maximum when ESRD develops. These findings mean that impaired red blood cell deformability could be pathogenic factors that are important for both the development of impairment in renal function. In other words, the impaired red cell deformability can be served as a maker for nephropathy in diabetic and non-diabetic patients, which are worthwhile to study further.

Acknowledgments

This work was supported by Grants from the SBD-National Core Research Center and Biorheology of NRL programs of KOSEF.

References

Bareford, D., P.C.W. Stone, N.M. Calwell, H.J. Meiselman and J. Stuart, 1985, Comparison of instruments for measurement of erythrocyte deformability, *Clinical Hemorheology* **5**, 311.

Baskurt, O.K., T.C. Fisher and H.J. Meiselman, 1996, Sensitivity of the cell transit analyzer (CTA) to alterations of red blood cell deformability: Role of cell size-pore size ratio and sample preparation, *Clinical Hemorheology* **16**, 753.

Brown, C., H. Ghali, Z. Zhao, L. Thomas and E. Friedman, 2005, Association of reduced red blood cell deformability with diabetic nephropathy, *Kidney International* **67**, 295.

Caimi, G. and R. Lo Presti, 2004, Techniques to evaluate erythrocyte deformability in diabetes mellitus, *Acta Diabetol* **41**, 99.

Chien, S., 1970, Shear dependence of effective cell volume as a determinant of blood viscosity, *Science* **168**, 977.

Dobbe, J.G.G., M.R. Hardeman, G.J. Streekstra and C.A. Grimbergen, 2004, Validation and application of an automated rheoscope for measuring red blood cell deformability distributions in different species, *Biorheology* **41**, 65.

Dobbe, J.G.G., G.J. Streekstra, M.R. Hardeman, C. Ince and C.A. Grimbergen, 2002, Measurement of the distribution of red blood cell deformability using an automated rheoscope, *Cytometry* **50**, 313.

Garnier, M., J.R. Attali, P. Valensi, E. Delatour-Hanss, F. Gaudey and D. Koutsouris, 1990, Erythrocyte deformability in diabetes and erythrocyte membrane lipid composition, *Metabolism* **38**,

794.

Hanss, M., 1983, Erythrocyte filterability measurement by the initial flow rate method, *Biorheology* **20**, 199.

Hardeman, M.R., P.T. Goedhart, J.G.G. Dobbe and K.P. Lettinga, 1994, Laser-assisted optical rotational cell analyser (LORCA): 1. A new instrument for measurement of various structural hemorheological parameters, *Clinical Hemorheology* **14**, 605.

Huang, Z., L. Hearne, C.E. Irby, S.B. King, S.K. Ballas and D.B. Kim-Shapiro, 2003, Kinetics of increased deformability of deoxygenated sickle cells upon oxygenation, *Biophysical Journal* **85**, 2374.

Macosko, C.W., 1993, Rheology: Principles, Measurements, and Applications. New York: VCH, 257.

Mauer, S.M. and B.M. Chavers, 1985, A comparison of kidney disease in type I and type II diabetes, *Adv. Exp. Med. Biol.* **189**, 200.

Porte, D. Jr. and M.W. Schwartz, 1996, Diabetics complications: Why is glucose potentially toxic?, *Science* **272**, 699.

Schmid-Schönbein, H., P. Ruef and O. Linderkamp, 1996, The shear strss diffractometer Rheodyn SSD for determination of erythrocyte deformability. I. Principle of operation and reproducibility, *Clinical Hemorheology* **16**, 745.

Schmid-Schönbein, H., R. Wells and R. Schildkraut, 1969, Microscopy and viscometry of blood flowing under uniform shear rate, *J. Appl. Physiol.* **26**, 674.

Shin, S., Y.H. Ku, M.S. Park and J.S. Jang, 2005, Rapid cell-deformability sensing system based on slit-flow laser diffractometry with decreasing pressure differential, *Biosensor and Bioelectronics* **20**, 1291.

Testa, I., S. Manfrini, F. Gregorio, A. Refe, A.R. Bonfigli, R. Testa and L. Piantanelli, 2003, Red blood cell deformability in diabetic retinopathy, *Biorheology* **32**, 389.

Usami, S., S. Chien and J.F. Bertles, 1975, Deformability of sickle cells as studied by microsieving, *J. Lab. Clin. Med.* **86**, 274.

Vaya, A., M. Martinez, J. Garcia, M. Labios and J. Aznar, 1992, Hemorheological alterations in mild essential hypertension, *Throm. Res.* **66**, 223.